

## A NUMERICAL ANALYSIS OF DETAILED ENERGY TRANSFERS IN ELASTIC-WAVE TURBULENCE

Naoto Yokoyama<sup>1</sup> & Masanori Takaoka<sup>2</sup>

<sup>1</sup>*Department of Aeronautics and Astronautics, Kyoto University, Kyoto, Japan*

<sup>2</sup>*Department of Mechanical Engineering, Doshisha University, Kyotanabe, Japan*

**Abstract** Triad interaction functions in elastic-wave turbulence are numerically investigated to show detailed energy transfers due to nonlinear interactions among wavenumbers. The energy exchange is active between the small-wavenumber stretching energy and the large-wavenumber kinetic energy. It is indicated that these nonlocal interactions carry the energy from the small-wavenumber forcing range to the large-wavenumber dissipation range.

### INTRODUCTION

Elastic waves propagating in a thin elastic plate exhibit turbulent properties when the degree of freedom is large, and then the system is called elastic-wave turbulence. In the elastic-wave turbulence, a (relatively) strongly nonlinear spectrum in small wavenumbers and the weakly nonlinear spectrum in large wavenumbers coexist. [1, 2] Despite the coexistence, the energy fluxes in both the strongly nonlinear regime and the weakly nonlinear regime are almost the same. [3] To see the energy transfers due to the nonlinear interactions among wavenumbers in more detail, the energy transfers are visualized by the triad interaction functions. The triad interaction functions represent the nonlinear energy transfer between kinetic energy of a wavenumber and stretching energy of another wavenumber by the medium of the other wavenumber. The mechanism of the energy transfer from a small-wavenumber energy-containing range to a large-wavenumber dissipation range is also discussed.

### RESULTS

The dynamics of elastic waves propagating in a thin plate is given by the Föppl-von Kármán (FvK) equation. Under the periodic boundary condition, the FvK equation is written as

$$\frac{d\zeta_{\mathbf{k}}}{dt} = \frac{p_{\mathbf{k}}}{\rho}, \quad \frac{dp_{\mathbf{k}}}{dt} = -\rho\omega_{\mathbf{k}}^2\zeta_{\mathbf{k}} + \sum_{\mathbf{k}_1+\mathbf{k}_2=\mathbf{k}} |\mathbf{k}_1 \times \mathbf{k}_2|^2 \zeta_{\mathbf{k}_1} \chi_{\mathbf{k}_2}, \quad \chi_{\mathbf{k}} = -\frac{E}{2k^4} \sum_{\mathbf{k}_1+\mathbf{k}_2=\mathbf{k}} |\mathbf{k}_1 \times \mathbf{k}_2|^2 \zeta_{\mathbf{k}_1} \zeta_{\mathbf{k}_2}, \quad (1)$$

where  $\zeta_{\mathbf{k}}$ ,  $p_{\mathbf{k}}$  and  $\chi_{\mathbf{k}}$  are the Fourier coefficients of the displacement, of the momentum, and of the Airy stress potential, respectively. The Young's modulus  $E$  and the density  $\rho$  are the material quantities of an elastic plate. The frequency  $\omega_{\mathbf{k}}$  is given by the linear dispersion relation,  $\omega_{\mathbf{k}} = (Eh^2/(12(1-\sigma^2)\rho))^{1/2} k^2$ , where  $\sigma$  and  $h$  are respectively the Poisson ratio and the thickness of the elastic plate.

The total energy of each mode  $E_{\mathbf{k}}$  is the sum of the kinetic energy  $K_{\mathbf{k}}$ , the bending energy  $V_{b\mathbf{k}}$ , and the stretching energy  $V_{s\mathbf{k}}$ , i.e.,  $E_{\mathbf{k}} = K_{\mathbf{k}} + V_{b\mathbf{k}} + V_{s\mathbf{k}}$ . [3] Here,  $K_{\mathbf{k}} = |p_{\mathbf{k}}|^2/(2\rho)$ ,  $V_{b\mathbf{k}} = \rho\omega_{\mathbf{k}}^2|\zeta_{\mathbf{k}}|^2/2$ ,  $V_{s\mathbf{k}} = k^4|\chi_{\mathbf{k}}|^2/(2E)$ . The total-energy transfer is also decomposed as  $T_{\mathbf{k}} = T_{K\mathbf{k}} + T_{V_{b\mathbf{k}}} + T_{V_{s\mathbf{k}}}$ , corresponding to each energy. The kinetic-energy transfer  $T_{K\mathbf{k}}$  is further decomposed to the second-order transfer and the fourth-order transfer. The second-order kinetic-energy transfer and the bending-energy transfer express the transmutation from kinetic energy to the bending energy and vice versa, hence the second-order kinetic-energy transfer and the bending-energy transfer cancel each other out. Therefore, the total-energy transfer is given as the sum of the the fourth-order kinetic-energy transfer and the stretching-energy transfer as  $T_{\mathbf{k}} = T_{K\mathbf{k}}^{(4)} + T_{V_{s\mathbf{k}}}$ , where

$$T_{K\mathbf{k}}^{(4)} = \frac{p_{\mathbf{k}}^*}{2\rho} \sum_{\mathbf{k}_1+\mathbf{k}_2=\mathbf{k}} |\mathbf{k}_1 \times \mathbf{k}_2|^2 \chi_{\mathbf{k}_1} \zeta_{\mathbf{k}_2} + c.c., \quad T_{V_{s\mathbf{k}}} = -\frac{\chi_{\mathbf{k}}^*}{2\rho} \sum_{\mathbf{k}_1+\mathbf{k}_2=\mathbf{k}} |\mathbf{k}_1 \times \mathbf{k}_2|^2 \zeta_{\mathbf{k}_1} p_{\mathbf{k}_2} + c.c. \quad (2)$$

The kinetic-energy transfer and the stretching-energy transfer due to a triad interaction with  $\mathbf{k}_1$  and  $\mathbf{k}_2$  are defined as

$$T_{K\mathbf{k}\mathbf{k}_1\mathbf{k}_2}^{(4)} = \frac{|\mathbf{k}_1 \times \mathbf{k}_2|^2}{2\rho} p_{\mathbf{k}} \chi_{\mathbf{k}_1} \zeta_{\mathbf{k}_2} \delta_{\mathbf{k}+\mathbf{k}_1+\mathbf{k}_2, \mathbf{0}} + c.c., \quad T_{V_{s\mathbf{k}\mathbf{k}_1\mathbf{k}_2}} = -\frac{|\mathbf{k}_1 \times \mathbf{k}_2|^2}{2\rho} \chi_{\mathbf{k}} \zeta_{\mathbf{k}_1} p_{\mathbf{k}_2} \delta_{\mathbf{k}+\mathbf{k}_1+\mathbf{k}_2, \mathbf{0}} + c.c. \quad (3)$$

The triad interaction function of the total energy is defined as  $T_{\mathbf{k}\mathbf{k}_1\mathbf{k}_2} = T_{K\mathbf{k}\mathbf{k}_1\mathbf{k}_2}^{(4)} + T_{V_{s\mathbf{k}\mathbf{k}_1\mathbf{k}_2}}$ . The triad interaction function  $T_{\mathbf{k}\mathbf{k}_1\mathbf{k}_2}$  is interpreted as the temporal rate of the energy increment at  $\mathbf{k}$  due to the interaction among the three wavenumbers  $\mathbf{k} + \mathbf{k}_1 + \mathbf{k}_2 = \mathbf{0}$ . The triad interaction function of the total energy satisfies the detailed energy balance:  $T_{\mathbf{k}\mathbf{k}_1\mathbf{k}_2} + T_{\mathbf{k}_1\mathbf{k}_2\mathbf{k}} + T_{\mathbf{k}_2\mathbf{k}\mathbf{k}_1} = 0$ . Namely, the triad interaction conserves the sum of the energies of the three wavenumbers.

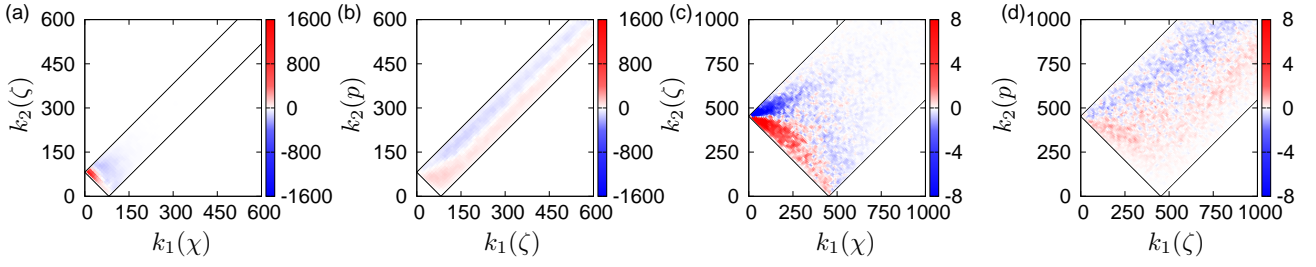


**Figure 1.** Azimuthally-integrated triad interaction functions of kinetic energy due to a triad interaction with  $k_1$  for  $\chi$  and  $k_2$  for  $\zeta$  (a, c), and stretching energy due to a triad interaction with  $k_1$  for  $\zeta$  and  $k_2$  for  $p$  (b, d). (a, b): for  $k = 26\pi$ , and (c, d): for  $k = 144\pi$ .

Because a triangle is determined by the lengths of the three sides, the azimuthally-integrated triad interaction functions in the statistically isotropic state are defined as

$$\mathcal{T}_K(k_1, k_2; |\mathbf{k}|) = (\Delta k)^{-2} \sum_{\substack{k_1 - \Delta k/2 \leq |\mathbf{k}'_1| < k_1 + \Delta k/2 \\ k_2 - \Delta k/2 \leq |\mathbf{k}'_2| < k_2 + \Delta k/2}} \langle T_{K\mathbf{k}\mathbf{k}'_1\mathbf{k}'_2} \rangle, \quad \mathcal{T}_{V_s}(k_1, k_2; |\mathbf{k}|) = (\Delta k)^{-2} \sum_{\substack{k_1 - \Delta k/2 \leq |\mathbf{k}'_1| < k_1 + \Delta k/2 \\ k_2 - \Delta k/2 \leq |\mathbf{k}'_2| < k_2 + \Delta k/2}} \langle T_{V_s\mathbf{k}\mathbf{k}'_1\mathbf{k}'_2} \rangle, \quad (4)$$

where  $\Delta k$  is the bin width to make the the azimuthal integration.

We performed a numerical simulation of the FvK equation (1), where the external forces and dissipation are added respectively in the small wavenumbers ( $|\mathbf{k}| \leq 8\pi$ ) and in the large wavenumbers (effective in the range  $|\mathbf{k}| \gtrsim 256\pi$ ). A statistically steady state is numerically obtained. In the statistically state, a (relatively) strongly nonlinear state in the small wavenumber and the weakly nonlinear state in the large wavenumbers coexist, where the separation wavenumber is roughly equal to 200.

Figure 1 shows the azimuthally-integrated triad interaction functions for  $k = |\mathbf{k}| = 26\pi$  and  $144\pi$ ; the former is in the strongly nonlinear small-wavenumber region, and the latter in the weakly nonlinear large-wavenumber region. Because of the triangle inequality, the azimuthally-integrated triad interaction functions are defined only in the rectangular domain. For  $k = |\mathbf{k}| = 26\pi$ , large magnitudes of the kinetic-energy transfer appear around the left corner, where the wavenumbers of  $\chi$  is small and the wavenumbers of  $\zeta$  is close to  $k$ . (Fig. 1(a)) Positive large values ( $\approx 1 \times 10^3$ ) are observed near the corner, while negative large values ( $\approx -1 \times 10^2$ ) in the region  $k_1 \approx k_2 \approx k$ . Note that the range of the color map is limited to the range from  $-1600$  to  $1600$  for visibility. Because the bending-energy transfer does not contribute to the energy budget among wavenumbers,  $\zeta(k_2)$  plays a mediating role. The local integral near the corner is positive. Therefore, the kinetic energy of  $k = 26\pi$  is transferred from the stretching energy of  $k_1 \ll k$ . Conversely, the triad interaction function of the stretching energy spreads over the rectangle domain, and the contribution from the large  $k_1$  and  $k_2$  is significant. (Fig. 1(b)) The positive values appear in the range  $k_1 > k_2 \gg k$ , while the negative values appear in the range  $k_2 > k_1 \gg k$ . Near the left corner  $k_1 \ll k$ , the triad interaction function of the kinetic energy for  $k = 144\pi$  has positive large values in the region  $k_2 < k$  of  $p$ , and negative large values in the region  $k_2 > k$ . (Fig. 1(c)) The triad interaction function of the stretching energy for the large wavenumbers has the significant contribution from the large  $k_1$  and  $k_2$  (Fig. 1(d)). Note that Figs. 1(a) and (b) and Figs. 1(c) and (d) are not substantially different, though the former wavenumber is taken from the strongly nonlinear regime, and the latter from the weakly nonlinear regime.

The results of the triad interaction functions shown in Fig. 1 can be understood by the detailed balance of the energy. The energy is transferred from the large-wavenumber kinetic energy to the small-wavenumber stretching energy, if the wavenumber of the kinetic energy is smaller than the wavenumber of the displacement that mediates the triad interaction. The energy is transferred from the small-wavenumber stretching energy, to the large-wavenumber kinetic energy if the wavenumber of the kinetic energy is larger than the wavenumber of the displacement. These nonlocal interactions between the small-wavenumber stretching energy and the large-wavenumber kinetic energy via the large-wavenumber displacement can carry the energy from the small-wavenumber forcing range to the large-wavenumber dissipation range. The energy transfer due to the nonlocal interactions will be compared with that due to the local interactions.

## References

- [1] Naoto Yokoyama and Masanori Takaoka. Weak and strong wave turbulence spectra for elastic thin plate. *Phys. Rev. Lett.*, **110**:105501, 2013.
- [2] Naoto Yokoyama and Masanori Takaoka. Identification of a separation wave number between weak and strong turbulence spectra for a vibrating plate. *Phys. Rev. E*, **89**:012909, 2014.
- [3] Naoto Yokoyama and Masanori Takaoka. Single-wave-number representation of nonlinear energy spectrum in elastic-wave turbulence of the Föppl–von Kármán equation: Energy decomposition analysis and energy budget. *Phys. Rev. E*, **90**:063004, 2014.